

# Development of silica based organic slurries for stereolithographic printing process

Frank B. Löffler<sup>a,\*</sup>, Ethel C. Bucharsky<sup>a</sup>, Karl G. Schell<sup>a</sup>, Stefan Heißler<sup>b</sup>, Michael J. Hoffmann<sup>a</sup>

<sup>a</sup> Institute for Applied Materials – Ceramic Materials and Technologies (IAM-KWT), Karlsruhe Institute of Technology (KIT), Haid-und-Neu-Str.7, 76131, Karlsruhe, Germany

<sup>b</sup> Institute of Functional Interfaces (IFG), Karlsruhe Institute of Technology (KIT), Hermann-von-Helmholz-Platz 1, 76344, Eggenstein-Leopoldshafen, Germany

## ARTICLE INFO

### Keywords:

Stereolithography  
Glass  
Suspension  
Polymerization kinetic  
Nanoparticles

## ABSTRACT

In this study, silica based slurries for stereolithographic printing of glass structures are developed and characterized. Stereolithography has the potential to print complex structures with high resolution. Therefore, acrylate based photocurable slurries have been developed and their viscosities are examined as a function of the solid loading. A critical shear rate can be derived, which must not be exceeded during the printing process. Therefore, rheological characterizations provide important insights into the printing process and the ability to produce samples with precise structures. Other properties such as polymerization time and curability kinetic were investigated with time dependent attenuated total reflection infrared spectroscopy (ATR-IR). Afterwards, the slurries were printed on a commercial printer operating with visible light. For debinding the printed green bodies, the decomposition temperatures were derived from thermogravimetric analysis in order to obtain stable and transparent samples.

## 1. Introduction

The term "additive manufacturing" is understood as the promise to design products of almost all material classes more and more individually. One method in the field of additive manufacturing is stereolithography, which was developed and patented by Chuck E. Hall in 1986 and is evolved till today. Meanwhile, many complex ceramic parts can be produced with this method [1,2]. Photocurable slurries based on a variety of different materials such as alumina, zirconia or tricalcium phosphate have been developed and marketed [3]. However, there are very few works on printing glass and glass structures.

Photocurable slurries are essential for the stereolithographic printing process. An acrylate based slurry with a certain photoinitiator content is the starting composition of most photosensitive slurries used in stereolithography. Wozniak et al. conducted rheological studies for a couple of slurries based on hydrophilic and non hydrophilic monomers such as butyl acrylate and 4 hydroxybutylacrylate and used amorphous silica as a glass former in the composition [4]. The group showed that the viscosity of silica based slurries strongly depends on the temperature of the slurries and the particle size of the used silica powder. They also found that there is a jump in viscosity at a certain shear rate. This critical shear rate depends on the solid loadings. Shear thickening behavior of fumed silica nanopowders in organic solvents at a critical

shear rate was previously investigated in detail by Raghavan et al. [5,6]. They found that the critical shear rate at which the thickening behavior sets in is lowered by increasing the silica concentration. An additional result is the finding that non polar butyl acrylate does not reach low viscosities even at low solid loading of the amorphous silica in the slurry [7]. The hydroxyl surface forms a solvation layer around the particles neglecting attractive van der Waals forces in organic matter. As a result, high particle concentrations can be dispersed by keeping the viscosity of the slurry low. The shear forces cause the slurry to reduce its viscosity until the critical shear rate is reached. Then the solvation layer collapses and hydration bonds form between the silica nanoparticles. This results in gelation of the slurry and an increase in viscosity.

Stereolithography offers great benefits in the field of rapid prototyping due to important factors that can be linked together: Free choice of shape, simultaneous manufacturing of multiple parts, little or no post processing steps and very high resolution of the parts. It has been shown that this technology can also be manufacture glass parts by the stereolithographic process [8]. Nevertheless, the polymerization process must be evaluated in detail depending on the printing parameters of commercial printers.

The aim of this research is the development of a silica based printable slurry composition which can be used in a commercial

\* Corresponding author.

E-mail address: frank.loeffler@kit.edu (F.B. Löffler).

**Table 1**Compositions of slurries with variation of SiO<sub>2</sub> solid loading.

	vol%	vol%	vol%	vol%	vol%
4-HBA	83.70	63.24	58.12	55.80	53.01
TEGDA	6.30	4.76	4.37	4.20	3.99
SiO <sub>2</sub>	10.00	32.00	37.50	40.00	43.00
CQ	Up to 1 wt% of 4-HBA content				
EDMAB	1:1 molar ratio to CQ				

stereolithographic printer. Therefore, slurries have been designed that consist of high solid loadings higher than 40 vol% and are suitable for use in stereolithography due to their adjusted properties.

## 2. Material and methods

At first, an organic dispersion medium was prepared. The monomer, 4 hydroxybutylacrylate (4 HBA, BASF, Germany) or hydroxyethylmethacrylate (HEMA, Sigma Aldrich, Germany), and the cross linker monomer, tetraethylenglycole diacrylate (TEGDA, Sigma Aldrich, Germany), were mixed up in a laboratory mixing system (Speedmixer®, Hausschild Engineering, Germany) at 1500 rpm for 30 s. HEMA and 4 HBA, whose use has already been described in literature, see ref. [7] and [9], are two acrylates with carbon chains of different lengths and a hydroxyl ending. Subsequently, SiO<sub>2</sub> nanoparticles, Aerosil OX50 with a specific surface (BET) of 35 65 m<sup>2</sup>/g (Evonik Degussa GmbH, Germany) [10], were stepwise dispersed using spin rates up to 2100 rpm for 30 s. To remove the air bubbles, the slurry is additionally mixed at low pressures of 100 mbar with the same spin rate for another minute. The compositions of the slurries are depicted in Table 1.

In addition to suspension properties such as stability and polymerization behavior it must be ensured that light scattering during exposure within the printing process is avoided as far as possible. Therefore, materials with similar refractive indices are needed. Aerosil OX50 has a refractive index (*n*) of 1.46 [11], 4 HBA with *n* = 1.454 [12] and TEGDA with *n* = 1.461 1.469 [13]. These *n* values are close to each other and therefore these materials seem to be suitable for preparing a printable silica slurry. An image of the suspension produced therewith is shown in Fig. 1 on the left side.

As photoinitiator camphorquinone, CQ (Merck, Germany), was used. Based on the mass of monomer, CQ was dispersed in the slurry. Ethyl 4(dimethylamino) benzoate, EDMAB (Sigma Aldrich, Germany), if used, was dissolved in the same step in a 1:1 equimolar ratio to CQ. The transparency of the slurries and the yellow shining of the CQ based slurry are shown in Fig. 1.

The viscosities of the slurries were measured at increasing shear rates up to 100 s<sup>-1</sup> at 20 °C (thermostatically controlled) with a rotation viscometer (HAAKE Mars Rheometer, Thermo Scientific, Germany).

The kinetic of the ongoing reactions were investigated by time resolved IR measurements. Therefore, a Bruker Tensor 27 FTIR

spectrometer with a Bruker Platinum ATR accessory (Bruker Optics, Germany) was used. Additionally, a LED Lamp (Thor Labs, Germany) with a wavelength of 455 nm was installed on top of the ATR crystal to cure the slurry during IR measurements.

The slurries were printed with a stereolithography printer (Cerfab 7500, Lithoz GmbH, Austria) which uses the bottom up method and operates at a wavelength of 460 nm. The light is split and focused by a digital micromirror device (DMD) allowing a layer by layer curing. The printer is able to print layer thicknesses between 25 and 100 μm with a lateral resolution of 40 μm minimum per pixel. The slurries were placed in the vat and pre sheared a few minutes before starting the printing process. All samples were printed with the same set of parameters: exposure time *t* = 24 s, intensity *I* = 5 mW/cm<sup>2</sup> corresponding to a total energy of 120 mJ/cm<sup>2</sup>.

To determine the parameters of the debinding process, simultaneous thermogravimetry differential scanning calorimetry measurements were performed by using a STA Jupiter F449 (Netzsch, Germany).

## 3. Results and discussion

### 3.1. Rheological behavior

In order to determine the viscosity of the suspensions and the behavior of the silica in the organic media, rheological measurements were performed. The monomer used in an SiO<sub>2</sub> based slurry forms a solvation layer around the surface of the nanoparticles [6]. The hydroxyl groups build hydrogen bonds to the silanol groups of the SiO<sub>2</sub> particles. In comparison to HEMA, 4 HBA has longer carbon chains, resulting in a higher viscosity of the slurry for comparable solid loading, as shown in Fig. 2. Comparing both slurries, it is detectable that the critical shear rate of the 4 HBA system is shifted to higher shear rates. The longer monomer chains act as steric repulsion forces between the nanoparticles, which decrease the probability of building hydrogen bonds between the silica nanoparticles and give a more stable slurry with a larger window of shear rates for processing.

Fig. 3 shows the viscosity as a function of shear rate for 4 HBA based slurries with various solid loading. As expected, the viscosity increases with increasing solid loading. The slurry containing only 32 vol% solid loading shows low viscosities even at low shear rates: 4 Pas at a shear rate of 1 s<sup>-1</sup> and 2 Pas at a shear rate of 10 s<sup>-1</sup>. By increasing the solid loadings to 37.5 vol% the viscosity rises up to 8 Pas at a shear rate of 10 s<sup>-1</sup> whereas for a 43 vol% the viscosity reaches 25 Pas. Despite the high viscosities, it is possible to use the slurry with high solid loadings for the printing process. Because of the shearing with the static wiper blade and the spin velocity of the vat, it is essential that the critical shear rate is as high as possible. The results show a decrease of the critical shear rate with increasing solid loadings. During the evaluation of process parameters, it was proved that slurries with the very high solid loadings of 43 vol% SiO<sub>2</sub> can be printed.

The rheological behavior of the slurries was studied in order to find an optimal solid loading and a suitable flow characteristic for the stereolithographic printing process. An adjusted viscosity and high critical



**Fig. 1.** Left: Slurry with 43 vol% Aerosil OX50, 53 vol% 4-HBA and 4 vol% TEGDA. Right: Same slurry additionally with 0.5 wt% CQ in relation to the main monomer 4-HBA and 1:1 equimolar EDMAB in relation to CQ which is shining yellow and can be seen in the online version (for interpretation of the references to colour in this figure legend, the reader is referred to the web version of this article).

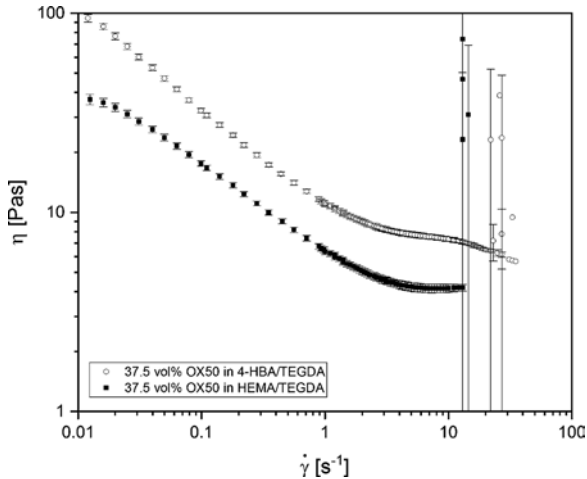


Fig. 2. Rheological behaviour of two slurries containing 37.5 vol% SiO<sub>2</sub> with two different monomers: The longer monomer 4-HBA and the shorter monomer HEMA. 4-HBA indicates higher viscosity values over the variation of the shear rate, but reaches a higher critical shear rate of about 25 s<sup>-1</sup>.

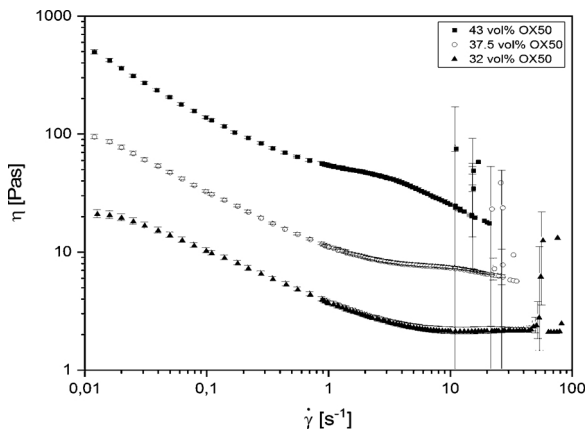


Fig. 3. Viscosities over shear rates of 4-HBA-based slurries with a variation of solid loadings: 32 vol%, 37.5 vol% and 43 vol%. The viscosity increases with rising solid loading and the critical shear rate shifts to lower shear rates.

shear rate, where shear thickening behavior starts, are very important for an effective printing process. The slurry is filled in the vat of the printer and is homogenized by shearing with a static wiper blade. When the shear rate exceeds the critical shear rate, the slurry collapses during homogenization. Therefore, the spin velocity of the vat must be adjusted, in order to obtain sharp edges of complex printed structures.

When the viscosity is low enough, which is up to 10 Pas, the slurry, which is not cured, can run off after the printing step. In opposite, high viscosities of more than 30 Pas can lead to curing of rests on the surface of the printed layer. As consequence a change of the printed structure occurs. Since the viscosity of the slurry strongly correlates with the solid loadings, the monomer and its interaction with the dispersed phase is decisive for the printing process.

Another interesting behavior of the slurries is their long time stability, that can be investigated using time dependent rheological measurements. Because of the critical shear rates of the slurries, a conventional oscillating rheological measurement is less suitable. For this reason, the slurry was examined by pre shearing and dwell time measurements. Fig. 4 shows viscosity values of a slurry with a high solid loading of 43 vol% SiO<sub>2</sub> measured at room temperature. The reference measurement was performed 24 h after the initial slurry was prepared. In the next step the slurry was pre sheared with the Speedmixer with 2100 rpm and 100 mbar for 30 s. Afterwards the viscosity of the slurry

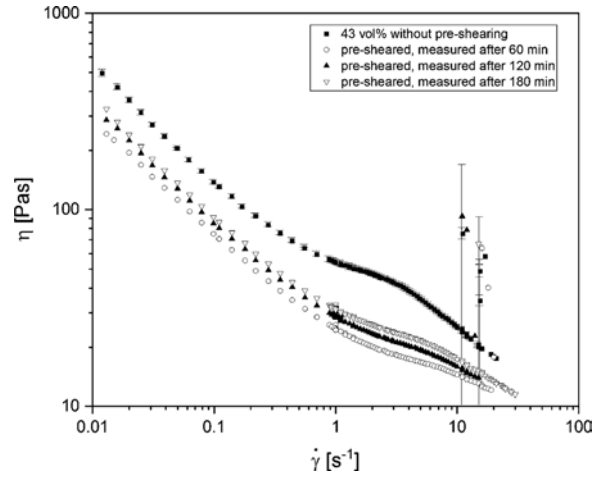


Fig. 4. Investigation of the viscosity of a 4-HBA-based slurry with a solid loading of 43 vol%. The reference viscosity curve was measured 24 h after preparation and was not pre-sheared. Afterwards the slurry was pre-sheared and the viscosity was measured after 60 min, 120 min and 180 min.

was measured subsequently after 60 min, 120 min and 180 min with the same measurement parameters. It shows that the viscosity of the slurry with 43 vol% solid loading without pre shearing reaches about 25 Pas at a shear rate of 10 s<sup>-1</sup>. The viscosity can be lowered with pre shearing to 15 Pas at a shear rate of 10 s<sup>-1</sup>. Moreover, it is necessary to homogenize the nanopowder in the polymeric surrounding without any sedimentation, keeping the viscosity values low. We observed that after a certain dwell time the viscosity increases again. This behavior indicates that the monomer probably sediment with time.

### 3.2. Investigations of curing kinetics

Photopolymerization is a time depending process, which is initiated by the radicalization of photoinitiators. These photoinitiators absorb photons upon irradiation of certain wavelength and form reactive species out of excited state, which initiate consecutive reactions. For our system we choose champherquinone (CQ) as a main photoinitiator and ethyl4 (dimethylamino)benzoate (EDMAB) as a co initiator. Fig. 5 shows the absorption spectrum of a slurry with 0.5 wt% CQ in a mixture of 4 HBA and TEGDA. The maximum absorbance is at a wavelength of about  $\lambda_{max} = 469$  nm, which is essential for the printing process with the Lithoz CeraFab 7500 owing a curing wavelength of 460 nm.

In order to determine polymerization kinetic parameters, time

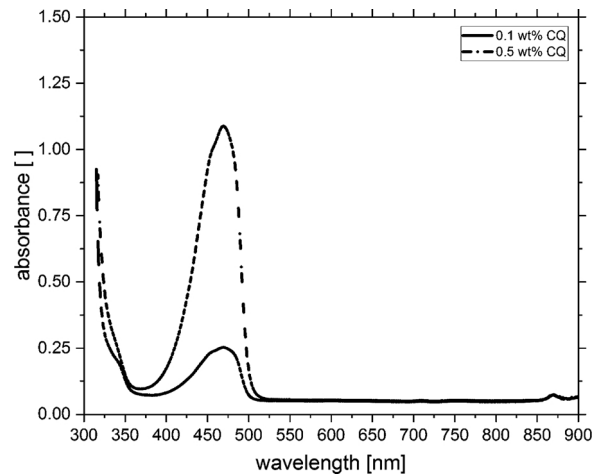


Fig. 5. Absorbance spectra of CQ in 4-HBA/TEGDA with 0.5 wt% and 0.1 wt% content. The absorbance maximum is at a wavelength of 469 nm.

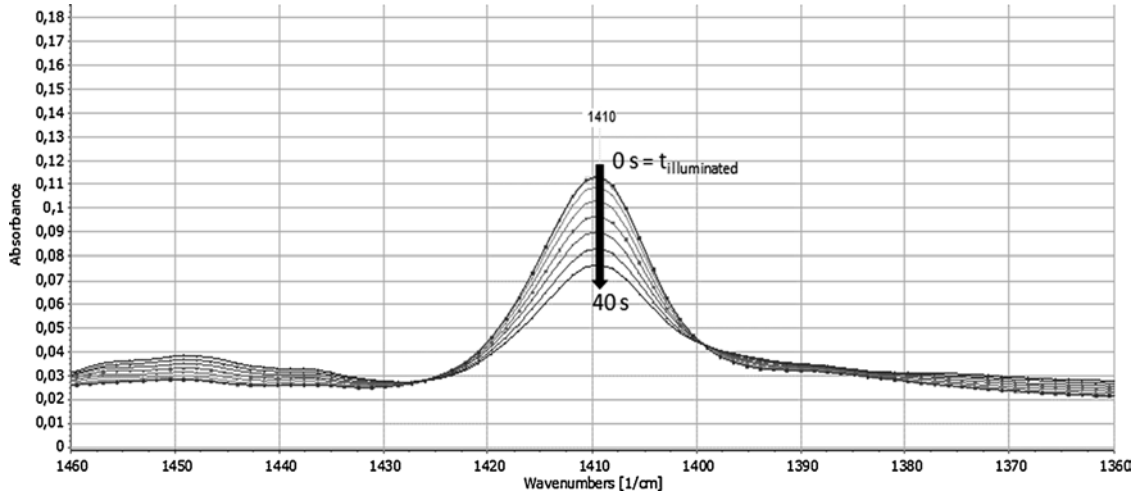


Fig. 6. IR spectra of 0.5 wt% CQ/EDMAB 40 vol% silica slurry illuminated with an intensity of 42 mW/cm<sup>2</sup>. At a wavenumber of 1410 cm<sup>-1</sup> the acrylate bond is measured and change its absorbance intensity during illumination. The peak with the maximum absorbance represents the slurry which was not illuminated in the beginning, the peak with the lowest absorbance intensity represents the slurry which was illuminated for 40 s. In between every four seconds a new IR spectrum during illumination was recorded.

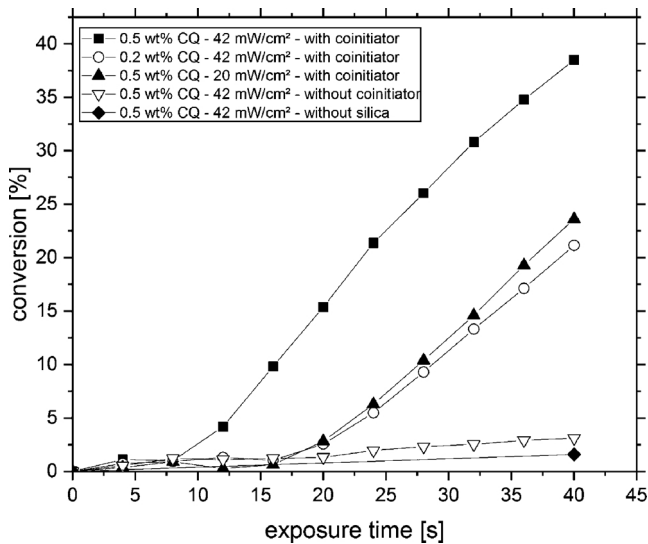


Fig. 7. Dependence of conversion on exposure time calculated from ATR-IR measurements.

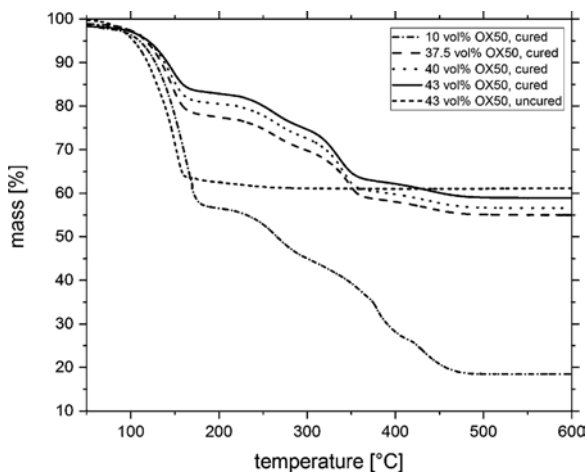


Fig. 8. TG analysis of printed samples with different solid content and a uncured slurry as a reference.

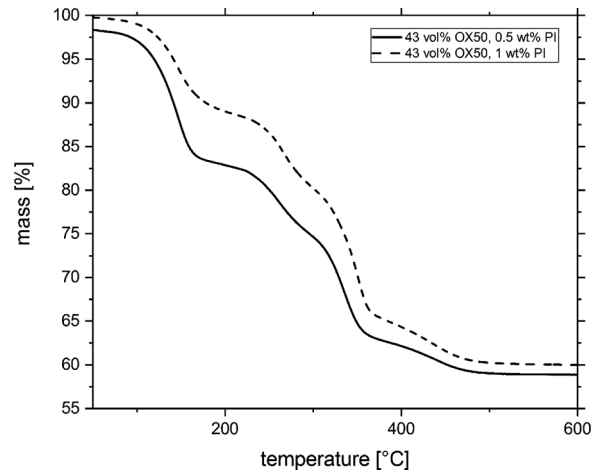
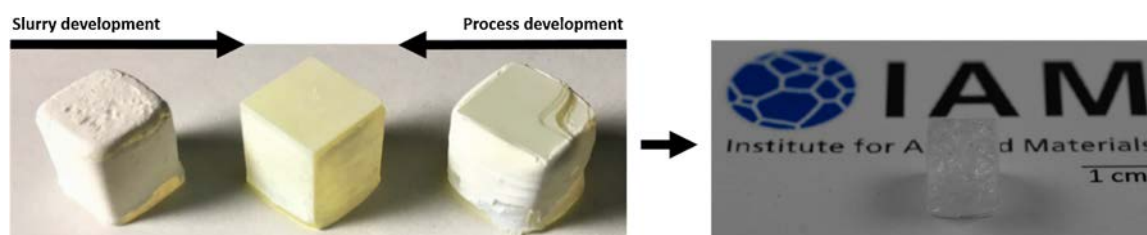


Fig. 9. TG analysis of two slurries containing 43 vol% SiO<sub>2</sub> and 0.5 wt% and 1 wt% CQ with 1:1 equimolar EDMAB.

depending IR measurements were performed. During the absorption measurement of ten spectra in 40 s, the slurry was illuminated with a LED with a wavelength of  $\lambda = 455$  nm as depicted in Fig. 6. The peak at a wave number of 1410 cm<sup>-1</sup> was identified as the acrylate (prop 2 enoates) bond which is radicalized and changes from a double to a single bond during illumination. The intensity of the peak decreases when the double bond breaks indicating the degree of the polymerization at a certain time. The change of the intensity related to the starting time is defined as a conversion value, which is shown in Fig. 7. The conversion is calculated from the integration of the peaks for all measurement over the 40 s exposure time.

A time delay of the conversion is observed when the slurry is cured. In order to obtain the kinetics for variations of photoinitiators concentration and exposure intensities slurries were tested as shown in Fig. 7. Slurries with a photoinitiator content of 0.5 wt% CQ with 1:1 equimolar content of EDMAB were exposed to an intensity of 42 mW/cm<sup>2</sup> showing a delay of about 7 s before the conversion starts. After 7 s the conversion increases approximately linear with the exposure time, reaching at 40 s a conversion of about 40 %. A delay time of 18 s is observed when the concentration of CQ is lowered to 0.2 wt% or when the exposure intensity is lowered to 20 mW/cm<sup>2</sup>. When the conversion starts, the slurries show in presence of CQ/EDMAB a similar trend as



**Fig. 10.** Stereolithographic printed cubes where the slurry and the printing process were developed. After printing with optimized parameters the cube was debinded and sintered to a cube of pure glass.

function of exposure time. This shows that the reaction rate can be adjusted via the photoinitiator content as well as via the lighting intensity.

In order to prove the relevance of the co initiator EDMAB, IR measurements of a slurry without EDMAB were performed. As observed from Fig. 7, no clear starting point of the conversion is recognizable. This indicates that the conversion increases very slowly with the exposure time in absence of EDMAB. To reach a fast polymerization EDMAB is needed as a co initiator. After CQ absorbs the light, a CQ radical is generated and the excited state of the CQ stands for about 20  $\mu$ s [14]. By using EDMAB as a co initiator, the excited state of CQ remains longer increasing the probability of exciting the acrylate and consequently the polymerization process increases. The concentration of the radicals in the system increases and the probability of the radicalization of the monomer rises significantly. Therefore, it is assumed that the step of the polymerization process is the radicalization of EDMAB out of CQ [15].

In our experiments, we found that the silica nanoparticles are necessary for initializing the polymerization process. As it is shown in Fig. 7, the polymerization does nearly not start in this 40 s of exposure time in the absence of SiO<sub>2</sub> nanoparticles. This is confirmed since only a small conversion is observed, even in the presence of 0.5 wt.% CQ and irradiation intensity of 42 mW/cm<sup>2</sup>. The assumption is that the influence of the silica in the system orders the acrylates while it is dispersed. The silica builds a shell of acrylates (solvation layer [6]) by ordering them around the surface where the hydroxyl group of the 4 HBA is bonded by van der Waals forces to the silanol groups of the surface of the silica particles. Cho et al. [16] found that the silica nanoparticles apparently accelerate the cure reaction due to a synergistic effect of silica nanoparticles during the photopolymerization process. The good linear correlation obtained supports the above assumption. More details on ongoing processes can be found in Cho et al. [17] where an assumption is given on how the addition of silica nanoparticles lowers the activation energy for UV curable acrylate polymerization processes.

### 3.3. Thermogravimetric analysis (TGA)

Next to the kinetics of the polymerization reactions, we analyzed the degree of polymerization of the cured samples after the slurry was stereolithographically printed. Therefore, TGA (thermogravimetric analysis) measurements of printed samples (small cylinders) were performed. Fig. 8 shows the mass loss for samples with different solid loadings during heating. For comparison an uncured slurry is measured as a reference as well. The uncured slurry has a massive mass loss between temperatures of 100–150 °C. Because of the missing polymerization, it is assumed that the monomer 4 HBA and the crosslinker TEGDA decompose completely in this temperature range. Otherwise, the polymerization leads to an increasing chain length during the printing process. Consequently, the decomposition temperature for polymerized parts are shifted to higher temperatures as can be seen in Fig. 8. Accordingly, some unpolymerized monomer remains in the samples. Samples with a similar solid content exhibit the same mass loss behavior due to the polymerization degree and the network composition. Only the curve of the slurry with 10 vol% SiO<sub>2</sub> shows a small

difference at temperatures around 400 °C, indicating a clear influence of the presence of the SiO<sub>2</sub> nanoparticles on the polymerization reaction.

In a further TG experiment the influence of the photoinitiator content on the composition of the printed sample was investigated. Fig. 9 gives the comparison of two slurries containing 0.5 wt% CQ and 1 wt% CQ. The most important difference between both curves is the mass loss at temperatures around 150 °C and 400 °C. The mass loss at 150 °C becomes smaller when the concentration of photoinitiator is higher. Hence, the content of residual monomer in the cured sample decreases.

The composition of the cured samples is changing by varying printing parameters or by different slurry compositions. Consequently, it is possible to adjust the slurry with e.g. a fixed photoinitiator content to reach a certain polymerization degree of the printed samples at certain printing parameters.

### 3.4. Thermal treatment

By developing the silica based suspension and the adjusted process parameter for printing this suspension, the accuracy of the geometry of the samples increases, as can be seen for a cube as a test geometry in Fig. 10 on the left side. The printed structures were debinded in a multi step temperature process up to 800 °C and were subsequently sintered at 1300 °C to reach a glassy structure (Fig. 10, right side).

## 4. Conclusion

This study shows results on slurry compositions based on silica for printing glass using a stereolithographic printing process. Its kinetic and printing parameters were investigated by time resolved IR measurements. Influences on the slurry viscosity as a function of solid loadings and dwell time after shearing were evaluated. In addition, with rheological measurements it was found that even at high solid loadings high critical shear rates are reached which allow the use of the slurry for the printing process. The measurements suggest that a delay of polymerization is dependent on the slurry composition and the exposure intensity. It was found that a certain concentration of EDMAB is necessary to initiate the polymerization process. On the other hand, it was observed that in absence of silica nanoparticles, no curing happens during illumination.

It is also proved with TG measurements that the composition of cured samples changes when the solid loading is varied. This could have a high influence on the debinding process where the polymer is burned out of the sample and should be taken into account.

### Declaration of competing interest

The authors declare that they have no known competing financial interests or personal relationships that could have appeared to influence the work reported in this paper.

### References

- [1] S. Gabriel, C.W. Hull United States Patent (19), (1984). doi:US005485919A.

- [2] J.W. Halloran, Ceramic Stereolithography: Additive Manufacturing for Ceramics by Photopolymerization, *Annu. Rev. Mater. Res.* 46 (2016) 19–40, <https://doi.org/10.1146/annurev-matsci-070115-031841>.
- [3] M. Schwentenwein, J. Homa, Additive manufacturing of dense alumina ceramics, *Int. J. Appl. Ceram. Technol.* 12 (2015) 1–7, <https://doi.org/10.1111/ijac.12319>.
- [4] M. Wozniak, T. Graule, Y. de Hazan, D. Kata, J. Lis, Highly loaded UV curable nanosilica dispersions for rapid prototyping applications, *J. Eur. Ceram. Soc.* 29 (2009) 2259–2265, <https://doi.org/10.1016/j.jeurceramsoc.2009.01.030>.
- [5] S.R. Raghavan, S.A. Khan, Shear-thickening response of fumed silica suspensions under steady and oscillatory shear, *J. Colloid Interface Sci.* 185 (1997) 57–67, <https://doi.org/10.1006/jcis.1996.4581>.
- [6] S.R. Raghavan, H.J. Walls, S.A. Khan, Rheology of silica dispersions in organic liquids: New evidence for solvation forces dictated by hydrogen bonding, *Langmuir* 16 (2000) 7920–7930, <https://doi.org/10.1021/la991548q>.
- [7] M. Wozniak, Y. de Hazan, T. Graule, D. Kata, Rheology of UV curable colloidal silica dispersions for rapid prototyping applications, *J. Eur. Ceram. Soc.* 31 (2011) 2221–2229, <https://doi.org/10.1016/j.jeurceramsoc.2011.05.004>.
- [8] F. Kotz, K. Arnold, W. Bauer, D. Schild, N. Keller, K. Sachsenheimer, T.M. Nargang, C. Richter, D. Helmer, B.E. Rapp, Three-dimensional printing of transparent fused silica glass, *Nature* 544 (2017) 337–339, <https://doi.org/10.1038/nature22061>.
- [9] F. Kotz, K. Plewa, W. Bauer, N. Schneider, N. Keller, T. Nargang, D. Helmer, K. Sachsenheimer, M. Schäfer, M. Worgull, C. Greiner, C. Richter, B.E. Rapp, Liquid glass: a facile soft replication method for structuring glass, *Adv. Mater.* (2016) 4646–4650, <https://doi.org/10.1002/adma.201506089>.
- [10] Evonik Industries, AEROSIL® OX 50 Hydrophile Pyrogenic Kieselsäure Produktinformation 5 (2013).
- [11] Aerosil–Pyrogenic Kieselsäuren Technical Overview, Evonik Industries, 1976, pp. 1–16.
- [12] 4-Hydroxybutyl Acrylate (4-HBA) Technical Information, BASF, 2015.
- [13] Tetra(ethylene Glycol) Diacrylate Technical Information, Sigma Aldrich, 2016, pp. 1–2.
- [14] J. Jakubiak, X. Allonas, J.P. Fouassier, A. Sionkowska, E. Andrzejewska, L.Å. Linden, J.F. Rabek, Camphorquinone-amines photoinitiating systems for the initiation of free radical polymerization, *Polymer (Guildf.)* 44 (2003) 5219–5226, [https://doi.org/10.1016/S0032-3861\(03\)00568-8](https://doi.org/10.1016/S0032-3861(03)00568-8).
- [15] J.P. Fouassier, J. Lalevée, Photoinitiators for polymer synthesis: scope, *React. Effic.* (2012), <https://doi.org/10.1002/9783527648245>.
- [16] J.D. Cho, H.T. Ju, J.W. Hong, Photocuring kinetics of UV-initiated free-radical photopolymerizations with and without silica nanoparticles, *J. Polym. Sci. Part A: Polym. Chem.* 43 (2005) 658–670, <https://doi.org/10.1002/pola.20529>.
- [17] J.D. Cho, Y.B. Kim, H.T. Ju, J.W. Hong, The effects of silica nanoparticles on the photocuring behaviors of UV-curable polyester acrylate-based coating systems, *Macromol. Res.* 13 (2005) 362–365, <https://doi.org/10.1007/BF03218467>.